Chen, and Crasemann[17] and fits best the theoretical data of these authors for $15 < Z < 70$. The values of Crone[15] for C, N, and O were determined relative to neon for which a theoretical value ($\omega_K = 8.1\times10^{-3}$) was used. A better value for neon seems to be that lying on the straight line ($\omega_K = 1.2\times10^{-2}$) in Fig. 1. Relative to this value Crone's results are $\omega_K = 1.3\times10^{-3}$, 2.2×10^{-3}, and 3.2×10^{-3} for C, N, and O, respectively, which fit the straight line more closely than the original values. The values for $Z = 13\cdots47$ from more recent and reliable measurements[18-23] fit this line best. Our results and those of Dick and Lucas[2] are close enough to the straight line so that one may say that Eq. (4) is a good approximation for the dependence of the K-shell fluorescence yield upon the atomic number at least down to $Z = 4$.

Thanks are due to J. Müller for help during the measurements and the synchrotron radiation group at DESY for their hospitality.

*Work supported by the Deutsche Forschungsgemeinschaft.

[1]E. J. McGuire, Phys. Rev. A 2, 273 (1970).
[2]C. E. Dick and A. C. Lucas, Phys. Rev. A 2, 580 (1970).
[3]W. Hink and H. Paschke, Phys. Rev. A 4, 507 (1971).
[4]A. J. Campbell, Proc. Roy. Soc., Ser. A 274, 319 (1963).
[5]R. Haensel and C. Kunz, Z. Angew. Phys. 23, 276 (1967).
[6]R. P. Godwin, in *Springer Tracts in Modern Physics, Ergebnisse der exacten Naturwissenschaft,* edited by G. Höhler (Springer, Berlin, 1969), Vol. 51, p. 1.
[7]R. Haensel and B. Sonntag, J. Appl. Phys. 38, 3031 (1967).
[8]D. Lemke and D. Labs, Appl. Opt. 6, 1043 (1967).
[9]B. L. Henke, R. White, and B. Lindberg, J. Appl. Phys. 28, 98 (1957).
[10]V. A. Fomichev and I. I. Zhukova, Opt. Spectrosk. 24, 284 (1968) [Opt. Spectrosc. (USSR) 24, 147 (1968)].
[11]R. Haensel, G. Keitel, B. Sonntag, C. Kunz, and P. Schreiber, Phys. Status Solidi (a) 2, 85 (1970).
[12]K. Feser, J. Müller, G. Wiech, and A. Faessler, J. Phys. (Paris), Colloq. 32, C4-331 (1971).
[13]K. Feser, thesis, Universität München, 1971 (unpublished).
[14]K. Feser, Rev. Sci. Instrum. 42, 888 (1971).
[15]W. Crone, Ann. Phys. (Leipzig) 27, 405 (1936).
[16]J. Byrne and N. Howarth, J. Phys. B: Proc. Phys. Soc., London 3, 280 (1970).
[17]V. O. Kostroun, M. H. Chen, and B. Crasemann, Phys. Rev. A 3, 533 (1971).
[18]L. E. Bailey and J. B. Swedlund, Phys. Rev. 158, 6 (1967).
[19]W. Bambynek, Z. Phys. 206, 66 (1967).
[20]W. Bambynek and D. Reher, Z. Phys. 214, 374 (1968).
[21]H. U. Freund, H. Genz, J. B. Siberts, and R. W. Fink, Nucl. Phys. A138, 200 (1969).
[22]J. Pahor, A. Kodre, M. Hribar, and A. Moljk, Z. Phys. 221, 490 (1969).
[23]C. Foin, A. Gidson, and J. Oms, Nucl. Phys. A113, 241 (1968).

rf Plasma Heating in a Mirror Machine at Frequencies near the Ion Cyclotron Frequency and its Harmonics*

D. G. Swanson and R. W. Clark
Electronics Research Center, The University of Texas at Austin, Austin, Texas 78712

and

P. Korn, S. Robertson, and C. B. Wharton
Laboratory of Plasma Studies, Cornell University, Ithaca, New York 14850
(Received 12 October 1971)

By applying 75 kW of pulsed rf power to a decaying hydrogen plasma following turbulent heating, we have maintained a plasma density of 10^{12} to 5×10^{12} cm^{-3} for the 600-μsec duration of the rf pulse. Neutral energy analyzer measurements of ion temperature indicate $T_i \sim 100$ eV, while diamagnetic loop measurements indicate 100 eV $< T_e + T_i <$ 200 eV. Probe measurements made using different equipment show discrete changes in the amplitude of the rf signals near the harmonics of the ion cyclotron frequency.

The purpose of the study reported here was to explore rf plasma heating at frequencies near the ion cyclotron frequency and its harmonics. Previous experiments reporting rf heating at harmonics of the ion cyclotron frequency either have been cursory with few details reported,[1] or were performed in a cold, low-density plasma with low rf power.[2] The results of this experiment show that it is possible to add energy to a collisionless plasma at densities as high as 5×10^{12}

cm^{-3}, that indeed the ions are heated, and that the hot plasma can be maintained for the duration of a 600-μsec rf pulse.

The plasma is injected into the THM-2 machine[3] along curved hexapole guide field rods from plasma guns located at each end of the device. The curved guide field sections, which reduce the number of neutrals entering the machine, terminate at a hollow, conical electrode at each end of the main vacuum chamber. The plasma column thus formed has a diameter of ~5 cm. The vacuum chamber is a 40-cm-diam, 200-cm-long stainless-steel cylinder. The pulsed mirror magnetic field for the THM-2 has a mirror ratio of about 1.9:1 with 150 cm between mirror peaks.

The rf power for the experiment was supplied by a 6-MHz, 75-kW amplifier in conjunction with a capacitive-impedance machine network. The rf antenna was a two-section Stix coil 18 cm long and 15 cm in diameter located 25 cm from the midplane. The antenna was left unshielded since earlier work has indicated that harmonic ion cyclotron effects are due to electrostatic waves,[4] and experiments have demonstrated that the harmonic effects disappear when a Faraday shield is used.[5]

Diagnostics consisted of an 8-mm zebra-stripe interferometer at the midplane, a diamagnetic loop 12.5 cm beyond the midplane on the opposite side from the antenna, and a neutral energy analyzer 12.5 cm beyond the diamagnetic loop. The forward and reflected rf power and the rf antenna current were also monitored.

The plasma column formed by the guns was preheated by turbulent heating. This produced a hot electron plasma which decayed with a time constant of about 50 μsec. When the rf heating was employed with the turbulent heating, the density and diamagnetic signals were maintained for the duration of the rf pulse. It was also observed that no heating of the gun plasma occurred when the turbulent preheating was not performed.

Heating was observed for a variety of confining magnetic field strengths ranging from low fields where both the second and third harmonics of the ion cyclotron frequency matched the rf frequency inside the machine, to higher fields where only the fundamental matched the rf frequency. Over this range, the points where the rf was resonant with the ion cyclotron frequency or its harmonics moved from near the minimum field point to the top of the mirror. The heating as determined from the diamagnetic loop was substantially the same for all of these conditions. Changing the magnetic field profile from the usual nearly parabolic profile to one that was nearly flat at the antenna with a shallow well and gentle beach near the diamagnetic loop also resulted in no significant increase in the diamagnetic loop signal. However, under all these conditions, the rf frequency matched the ion cyclotron frequency or one of its harmonics at some point in the machine. Because of equipment and time limitations, it was not possible to operate the 75-kW transmitter under conditions where neither the fundamental nor harmonics of the ion cyclotron frequency matched the rf frequency at any point in the machine. However, some rather cursory wave measurements, which have been made with different equipment at a lower frequency, indicate a magnetic field dependence. These latter measurements were made at 4 MHz using a spark gap and capacitor arrangement designed to ring with the antenna inductance. An electrostatic probe was used to measure rf fluctuations inside the plasma. For these experiments a distance of 75 cm separated the antenna and probe. In this configuration, the magnetic field strength at the antenna was the same as that at the probe, about 20% above the field strength at midplane. The rf signal measured with the electrostatic probe decreased in steps as the magnetic field was increased, with the steps occurring very near the harmonics and fundamental of the ion cyclotron frequency. Below the ion cyclotron frequency the rf signal measured was only about 17% of the signal measured above the second harmonic, and the antenna loading, as deduced from the decay time of the envelope of the rf ringing, was significantly reduced.

In Fig. 1 we present an example of the data collected for each shot using the 75-kW rf transmitter. The time scale is 100 μsec/division for all traces. Traces a and b indicate the forward and reflected power measured by square-law detectors, where 5 divisions correspond to 100 kW. Trace c shows the corresponding diamagnetic signal. The base-line slope results from the diamagnetic loop being not completely compensated for changes in the confining magnetic field. The calibration of the diamagnetic loop signal, using a 1-msec integrator, and assuming that the plasma is uniform over the 150 cm between the mirrors, is 1 J of perpendicular energy per division. This trace (c) shows that when rf is applied after the energy due to turbulent heating has decayed to about 0.46 J (in 100 μsec), the level is maintained for the duration of the pulse.

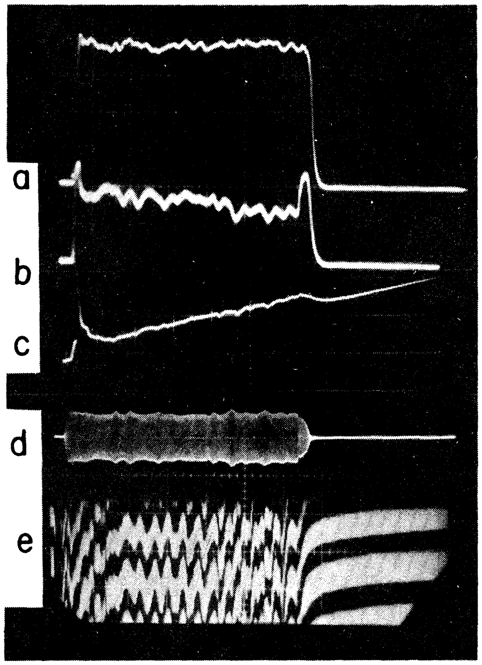

FIG. 1. Oscilloscope traces showing data collected on each shot. Trace a, incident rf power; b, reflected rf power; c, diamagnetic loop; d, antenna current; e, 8-mm interferometer.

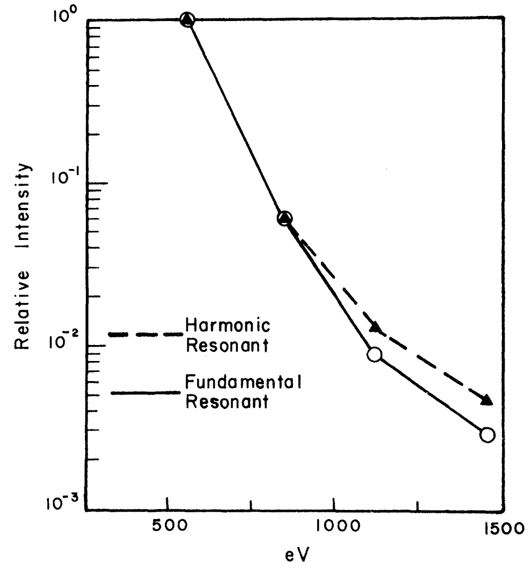

FIG. 2. Results of neutral energy-analyzer measurements. Measurements taken 550 μsec after the start of the rf pulse.

While the general level of the diamagnetic signal is typical, some exhibit a slowly growing level or a slowly decaying level.

In trace d we display the antenna current which is generally a good indication of net power input. The fluctuations in current amplitude are seen to correlate with fluctuations in the diamagnetic signal. These indicate some fluctuations in the plasma conditions which lead to variable loading of the antenna. The most obvious indication of fluctuations in plasma conditions is seen in the 8-mm interferometer display.[3] The interpretation of this display depends on the radial density profile, which we will take to be approximated by a cosine curve that vanishes at the antenna radius. With this assumption, a phase shift giving one full fringe displacement corresponds to a peak density of 2.4×10^{12} cm^{-3}. This example corresponds on the average to about 3.1×10^{12} cm^{-3}, but late in time the fluctuations suggest peak densities 2–3 times the average value. The frequency of these fluctuations was generally in the 20- to 40-kHz range, and for this example can be seen to vary from about 28 kHz to below 25 kHz. While the exact nature of the low-frequency fluctuations remains obscure, their appearance on the diamagnetic loop suggests that longitudinal bunching may be occurring. Furthermore, the mirror bounce frequencies are in the right frequency range to account for such bunching. However, the possibility of rotational or radial bunching cannot be discounted. The fluctuations are apparently driven by the rf since they stop abruptly at the end of the rf pulse.

One final conclusion that can be deduced from the data shown in Fig. 1 (assuming a cosine radial density distribution) is that $T_e + T_i \sim 120$ eV. From many such pictures at various power levels, the range of the temperatures from diamagnetic loop measurements is 100 eV $\lesssim T_e + T_i \lesssim$ 250 eV.

The energy analysis of fast neutral atoms (from charge exchange) shown in Fig. 2 indicates the ion energy distribution. The measurements were made with a neutral-atom stripping analyzer similar to that described by Jensen and Scott[6] and by Fleischmann and Tuckfield[7] but having only 30° of electrostatic deflection instead of the usual 120°. The smaller angle gives increased signal but reduces the energy resolution ($\Delta E/E = 0.4$).

Because of uncertainty in the calibration of the analyzer and its sensitivity to impurity atoms, it was used only for relative measurements. At the end of the 600-μsec pulse, the slope between data points at 560 and 840 eV indicates an ion temperature of 108 eV when the second harmonic is resonant and 104 eV when the fundamental is resonant, which are the same values within experimental error. It is apparent in both cases that the distribution in non-Maxwellian with a higher-energy tail.

It was noted in the measurements that the neutral signals did not show the fluctuations observed in the other diagnostics. This may result from the neutral detector accepting only these ions with $V_{i\parallel} \ll V_{i\perp}$, as a result of the small input angle of the analyzer. Thus, any ions oscillating longitudinally between the mirrors would have too large a parallel velocity when passing the analyzer port unless their turning point were at the analyzer port. The conclusion from the neutral analyzer data is that the ions are being heated, but the uncertainty in the density profile and corresponding uncertainty in the interpretation of the diamagnetic signals makes it impossible to prove that $T_i > T_e$. It is probable, however, that T_i is of the order of, or greater than, T_e.

An important consideration in plasma heating is to determine whether a saturation has been reached and if the attainable temperatures are limited. From the fact that the diamagnetic loop signals were essentially level in time, we conclude that the power input was balanced by the energy loss rate and that this condition was reached quickly. As the power level was changed, however, the energy level changed, as shown in Fig. 3. We see that there was generally a linear relation between plasma energy and net power and little difference between the case where the fundamental is resonant with the rf and the case where the harmonic is resonant. We conclude that if a limit to the plasma heating exists, it is above the power levels attained in this experiment. We also note that the average density was nearly independent of net power, so we conclude that the temperature is nearly proportional to net power.

Depending on rf impedance matching and other conditions within the plasma, the maximum incident power to the antenna was ~78 kW, and the minimum reflected power was ~2 kW. More typical values are 64–68 kW incident and 4–8 kW reflected, yielding an average power transfer efficiency of ~90%. Assuming equilibrium between net power input and energy-loss rates estimated from diamagnetic signal decay yields overall power transfer efficiencies between 20% and 40%.

It is not entirely clear from the data taken up to this point whether the increase in the length of time that the plasma was maintained, when the rf heating was employed, was due to rf ionization or to an increase in the containment time as a result of particles being driven away from the mirror loss cones by the rf heating. Some evidence exists to support either hypothesis; however, none of it is conclusive. Future experiments are planned to try to resolve this question.

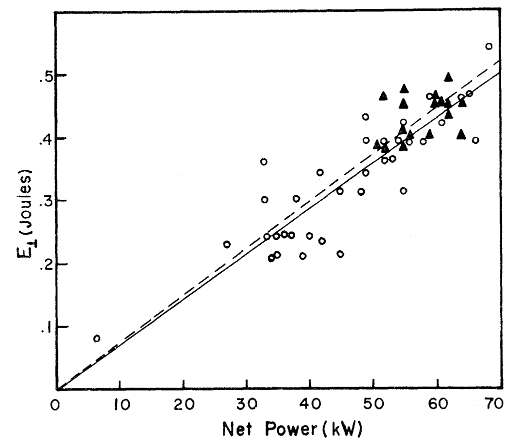

FIG. 3. Perpendicular plasma energy plotted against net rf power transferred to the plasma. Circles, shots where only the fundamental cyclotron frequency was resonant; triangles, present shots where the second and third harmonics were resonant. Least-squares fits for the two cases are shown.

We conclude from the somewhat incomplete data that the observed rf heating results from electrostatic waves propagating and damping near the ion cyclotron frequency and its harmonics. The two likely candidates are the electrostatic ion cyclotron (EIC) wave and the quasi ion Bernstein (QIB) wave, both of which propagate and damp near harmonics of the ion cyclotron frequency. The QIB wave requires $\omega/k_\parallel V_e \gg 1$ for weak electron Landau damping, which implies the machine is about a half wavelength long. For weak electron Landau damping the EIC wave requires $\omega/k_\parallel V_e \ll 1$ which for $T_e \sim 100$ eV implies a wavelength parallel to the magnetic field on the order of or less than 10 cm. In addition, the linear theory for the EIC wave requires $T_e \gg T_i$, which probably is not satisfied in the experiment for times greater than perhaps 20 μsec after the turbulent heating is over. When finite-amplitude effects are considered, however, the role of Landau damping is less clear, so that either wave might propagate, and the wavelength estimates may be invalid. Indeed, either or both waves could have been launched by the unshielded Stix coil. Future experiments are planned in which the wave and resonance conditions will be stuided more thoroughly and which should resolve some of these uncertainties.

*Research supported by the U. S. Atomic Energy Commission.

[1]S. Yoshikawa, M. A. Rothman, and R. M. Sinclair, Bull. Amer. Phys. Soc. 10, 509 (1965).

[2]M. Kristiansen and A. A. Dougal, Phys. Fluids 10, 596 (1967).

[3]C. B. Wharton, P. Korn, and S. Robertson, Phys. Rev. Lett. 27, 499 (1971); C. B. Wharton *et al.*, in Proceedings of the Fourth International Atomic Energy Agency Conference on Plasma Physics and Controlled Nuclear Fusion Research, Madison, Wisconsin, 1971 (to be published).

[4]D. G. Swanson, Phys. Fluids 10, 1531 (1967).

[5]N. Dodge, Ph. D. thesis, The University of Texas at Austin (unpublished).

[6]T. H. Jensen and F. R. Scott, Phys. Fluids 11, 1809 (1968).

[7]H. H. Fleischmann and R. G. Tuckfield, Jr., Nucl. Fusion 8, 81 (1968).

Molecular Dynamics of the Widom-Rowlinson Parallel Hard-Square Model*

H. L. Frisch and C. Carlier
State University of New York at Albany, Albany, New York 12203
(Received 9 February 1972)

Molecular dynamics of a Widom-Rowlinson mixture of type-1 and -2 parallel hard squares appears to reveal a (first order) phase transition with plait point at density $\rho_1 = 0.74$ of type-1 particles.

Widom and Rowlinson[1] have investigated a true continuum model which exhibits a phase transition that has an underlying symmetry closely analogous to the hole-particle symmetry of the lattice gas. In this model there are two kinds of particles, type 1 and type 2. The only interac-

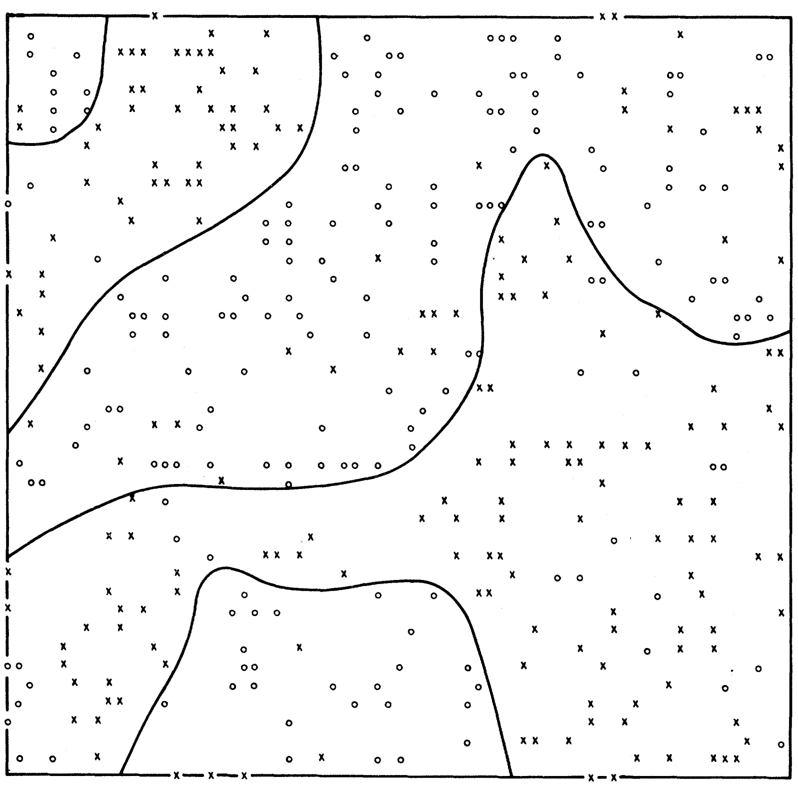

FIG. 1. Snapshot of a system of 200 type-1 particles and 200 type-2 particles, after 18 000 collisions at $\tau = 1.8$ ($\tau = 4/\rho$). "Boundaries" separating phase domains are indicated. The printout resolution of the location of the centers of the particles as given to 71 intervals along the horizontal axis and 42 intervals along the verticle axis.

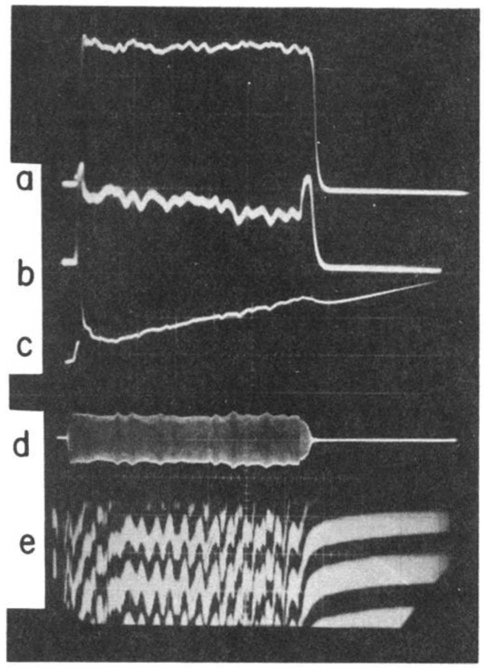

FIG. 1. Oscilloscope traces showing data collected on each shot. Trace *a*, incident rf power; *b*, reflected rf power; *c*, diamagnetic loop; *d*, antenna current; *e*, 8-mm interferometer.